Materials Research Proceedings **17** (2020) 132-137 https://doi.org/10.21741/9781644901038-20

The Influence of Plasma Cutting Parameters on the Geometric Structure of Cut Surfaces

RADEK Norbert[1, a *], PIETRASZEK Jacek [2,b], RADEK Mateusz [3,c] and PARASKA Olga[4,d]

[1]Kielce University of Technology, Faculty of Mechatronics and Mechanical Engineering,Al. 1000-lecia Państwa Polskiego 7, 25-314 Kielce, Poland

[2]Cracow University of Technology, Institute of Applied Informatics, Faculty of Mechanical Engineering, Al. Jana Pawła II 37, 31-864 Cracow, Poland

[3]The Catholic Public Middle School, Stanisława Kostki 17, 25-341 Kielce, Poland

[4]Khmelnitskiy National University, Department of Chemical Technology, Instytutska 11, 29016, Khmelnickiy, Ukraine

[a] norrad@tu.kielce.pl, [b] jacek.pietraszek@mech.pk.edu.pl, [c] mateusz6676@wp.pl, [d] olgaparaska@gmail.com

Keywords: Plasma Cutting, Surface Geometric Structure, Various Materials

Abstract. The paper presents the results of microgeometry measurements of cut surfaces. The cutting was carried out using a Hypertherm hand plasma cutter. Samples made of copper, 0H18N9 stainless steel and S355E low-alloy steel were the used tests. The current values at which the smallest roughness of the cut surface was obtained for a given material were determined.

Introduction

In modern industries, technologies using a concentrated energy stream are increasingly dominating [1-4]. These technologies include, among others, the plasma cutting method, which, due to high technological capabilities and low operating costs, is one of the most common thermal cutting processes [5, 6].

Plasma arc cutting, commonly known as plasma cutting, is a modification of the GTA plasma welding process. Plasma cutting was introduced to the industry in the 1950s to enable cutting of corrosion resistant steels and independent metals. The plasma cutting process involves melting and removing metal from the cutting gap with a highly concentrated plasma electric arc glowing between the non-fusible electrode and the workpiece. In a plasma electric arc, gas is strongly ionized with a high concentration of kinetic and thermal energy. Then the gas travels from the plasma nozzle, narrowing towards the cutting gap, at a speed close to the speed of sound. The temperature of the plasma stream is in the range of 10,000÷30,000 K and depends on the current intensity, the degree of arc narrowing and the type and composition of plasma forming gas [5].

It is possible to cut all electrically conductive construction materials. Non-metallic materials can only be cut with independent arc plasma torches. Unlike oxygen cutting, plasma cutting allows for cutting materials such as aluminum and its alloys as well as high-alloy steels [7].

The plasma cutting process is used for manual, mechanized and robotic cutting of steel and independent metals at high speeds in all positions. Thanks to the high temperature of the plasma arc, cutting begins immediately, without heating. The disadvantage of the process is very high noise levels, electric shock hazard, strong arc light radiation, large amounts of gases and fumes.

Materials Research Proceedings **17** (2020) 132-137 https://doi.org/10.21741/9781644901038-20

Currently, a dynamic development of hand-held devices and numerical machines for plasma cutting is observed. The main development directions concern improvement of technical parameters of cutting devices, obtaining high quality of cutting surface and increasing cutting accuracy [8, 9]. It may be of particular interest in the preparation of hydraulic accessories requiring high tightness [10-12], difficult-to-cut materials [13-15] and precise processing of smart plates [16, 17]. This method of cutting should significantly reduce the number of failures and non-conformities, which will affect the efficiency of management systems [18, 19]. Thanks to the cutting with minimal heating, damage leading to corrosion is avoided, which may be beneficial in the production of agricultural machinery parts that are exposed to contact with chemically aggressive biological agents [20]. Last but not least, plasma cut edges have a very interesting geometry and microstructure, which should inspire the development of theoretical and practical image analysis methods used in materials science [21, 22].

Materials and cutting parameters

50 x 5 x 250 mm samples made of copper, 0H18N9 stainless steel and S355E low-alloy steel were the subject of the study. Five samples of each of the aforementioned material were prepared for testing. The thermal cutting was carried out on a stand with a Hypertherm mechanized plasma cutter, model Powermax 1650. The plasma cutting holder was guided by a welding carriage. The scheme of the plasma cutting process is shown in Fig.1. The cutting parameters were selected experimentally. The following parameter values were adopted:

– cutting speed 0.8 m/min (for 0H18N9 and S355E steel) and 0.5 m/min (for copper),
– cutting current 40÷80 A,
– 60% duty cycle,
– plasma gas - air with a pressure of 0.62 MPa,
– rated air flow of 250 l/min.

The cut samples were subjected to the following tests:

– observation of cut surfaces with a stereoscopic microscope,
– microgeometry measurements.

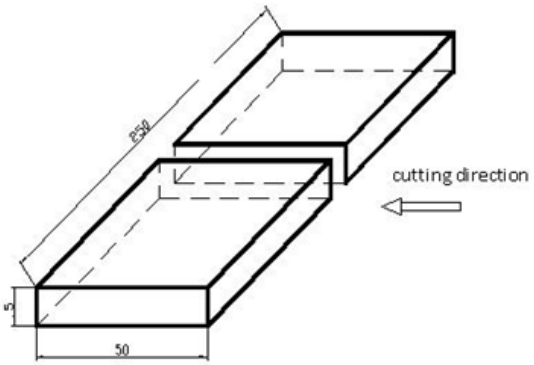

Fig. 1. The scheme of the plasma cutting process

Results and discussion

Surface geometric structure (SGS) substantially influences many processes that occur in the outer layer. A lot of publications deal with measurement methods and the assessment of surface roughness and waviness [23, 24].

Measurements of surface geometric structure were carried out at the Laboratory of Computer Measurements of Geometric Quantities of the Kielce University of Technology.

Materials Research Proceedings **17** (2020) 132-137 https://doi.org/10.21741/9781644901038-20

Selected results of microgeometry measurements for individual materials are presented in the form of graphs, which are presented in Figures 2÷4. Exemplary protocols for measuring the microgeometry parameters of the tested samples are presented in Figures 5÷7.

Figure 2 shows that the smallest roughness of the cut surface was obtained at a cutting current of I = 70 A and was Ra = 7.76 μm, the largest roughness was obtained at a current I = 40 A and was Ra = 13.7 μm.

In the case of cut samples of OH18N9 stainless steel, it appears that the smallest roughness of the cut surface Ra = 20.2 μm was obtained at a cutting current of I = 60 A (Fig. 3). The largest roughness of the cut surface was created at the current I = 50 A and was Ra = 27.7 μm.

While analyzing Figure 4, it was found that the smallest roughness of the cut surface was obtained at a cutting current of I = 60 A where the roughness was Ra = 2.95 μm, and the largest Ra = 13.1 μm at a cutting current of I = 40 A.

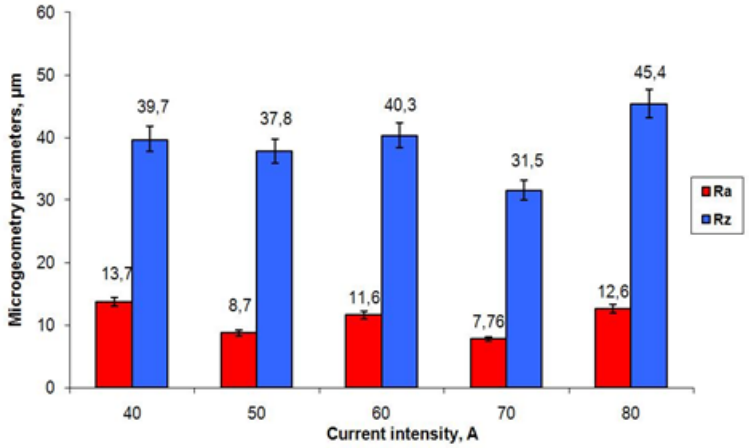

Fig. 2. Selected microgeometry parameters for copper samples

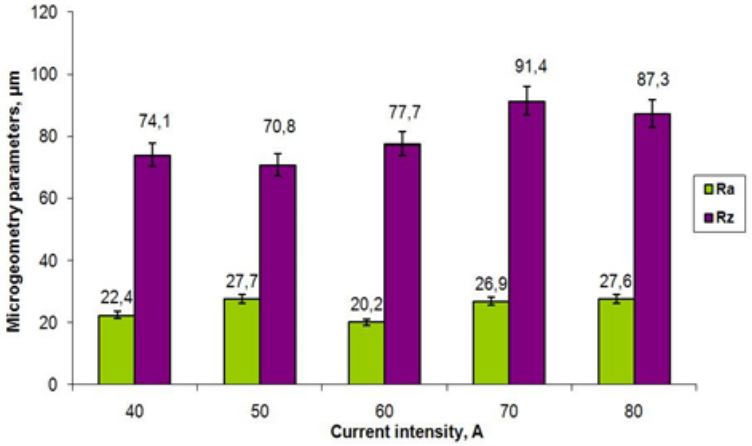

Fig. 3. Selected microgeometry parameters for 0H18N9 steel samples

From the graphs presented in Fig.2, Fig.3 and Fig.4, we can read that the smallest values of roughness of the cut surfaces of the tested materials occur at a cutting current of 60 to 70 A.

In the further part of the research, stereoscopic observations of the cut surfaces were made using a set consisting of an OLYMPUS stereoscopic microscope and a digital camera. Examples

Materials Research Proceedings **17** (2020) 132-137 https://doi.org/10.21741/9781644901038-20

of photographs of cut surfaces of samples of copper, OH18N9 stainless steel and S355E low-alloy steel are presented in Figures 5a–5c.

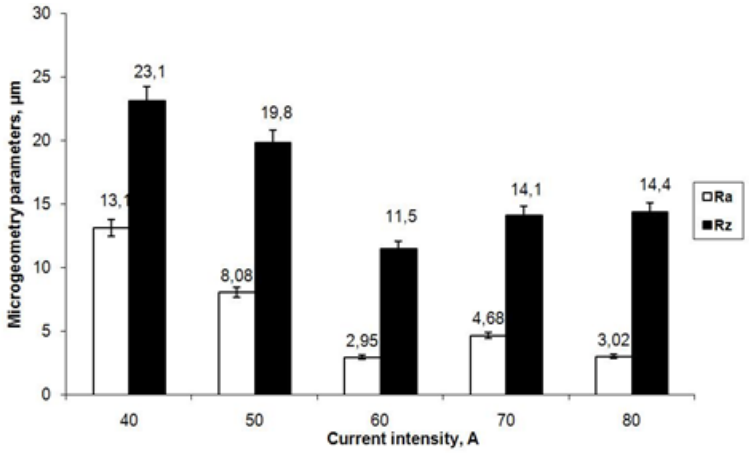

Fig. 4. Selected microgeometry parameters for S355E steel samples

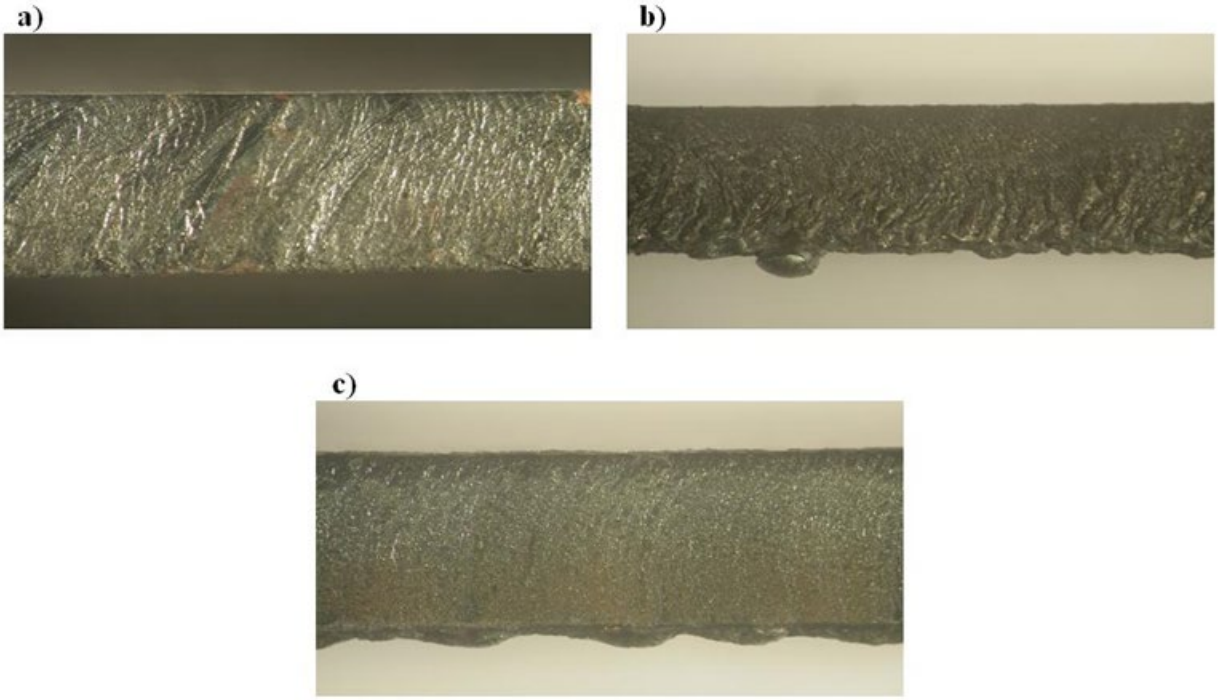

Fig. 5. Stereoscopic photographs of surfaces cut with plasma (x8 magnification): a) sample from Cu - I = 60 A, b) sample of OH18N9 steel - I = 40 A, c) sample of S355E steel - I = 80 A

While analyzing stereoscopic photographs of cut surfaces, we can observe that at a cutting current of 80 A, the copper sample is not cut, only melted. The lower edge shows the oxidized form and slag. By reducing the current to 70 A, we get a cutting surface with a lower roughness with a small amount of slag on the bottom edge. The most accurate surface was obtained at a

current of 60 A. A reduction of the cutting current to 50 A caused the cut surfaces to be characterized by considerable unevenness. At 40 A, the material was not cut completely.

When analyzing stereoscopic photographs of cut surfaces of OH18N9 steel samples, we can see that the most favorable surface quality effect occurred when cutting the material at a current of 40 A.

However, observing stereoscopic photographs of the cut surfaces of S355E steel samples, we can conclude that the best cutting results were obtained at a current of 80 A. The most adverse cutting occurred at a current of 50 A, as evidenced by slag on the lower edge of the cut surface.

Summary

The lowest roughness values of the cut surfaces of samples of copper, OH18N9 steel and S355E steel were obtained at a current of 60÷70 A. While analyzing stereoscopic photographs of the cut surfaces of the samples, we can see traces of cut in the form of oblique grooves and a characteristic slag overhang on the bottom edge of the cut material. When assessing the geometric structure of the cut surfaces, at a later stage of the study, chemical composition and structural changes that occur in the material as a result of the plasma arc should be performed. It also seems advisable to take measurements of the cut surface hardness and the heat affected zone.

References

[1] N. Radek, K. Bartkowiak, Laser treatment of electro-spark coatings deposited in the carbon steel substrate with using nanostructured WC-Cu electrodes, Physics Procedia 39 (2012) 295-301. https://doi.org/10.1016/j.phpro.2012.10.041

[2] P. Kurp, D. Soboń, The influence of laser padding parameters on the tribological properties of the Al2O3 coatings, METAL 2018 27th Int. Conf. Metallurgy and Materials, Ostrava, Tanger, 1157-1162.

[3] N. Radek, Determining the operational properties of steel beaters after electrospark deposition, Eksploatacja i Niezawodność – Maintenance and Reliability 4 (2009) 10-16.

[4] A. Gądek-Moszczak, N. Radek, S. Wroński, J. Tarasiuk, Application the 3D image analysis techniques for assessment the quality of material surface layer before and after laser treatment, Advanced Materials Research 874 (2014) 133-138. https://doi.org/10.4028/www.scientific.net/AMR.874.133

[5] A. Klimpel, Welding and cutting of metals, Warszawa, WNT, 1999.

[6] J. Czech, J. Dworak, Welding plasma techniques in the domestic industry, Bulletin of the Welding Institute 5 (1995) 54-55.

[7] T. Pfeifer, Plasma cutting of high-alloy steel, Polish Welding Review 4 (2001) 15-19.

[8] T. Pfeifer, Modern systems of automated plasma cutting, Polish Welding Review 7-8 (2000) 22-25.

[9] ZAKMET company homepage – plasma, oxygen, laser CNC cutting. http://www.zakmet.pl (access 23.04.2020)

[10] P. Walczak, A. Sobczyk, Simulation of water hydraulic control system of Francis turbine. Proc. 8th FPNI Ph.D Symposium on Fluid Power, 2014, art. V001T04A001. https://doi.org/10.1115/FPNI2014-7814

[11] M. Domagala, H. Momeni, J. Domagala-Fabis, G. Filo, D. Kwiatkowski, Simulation of cavitation erosion in a hydraulic valve. Materials Research Proceedings 5 (2018) 1-6. https://doi.org/10.21741/9781945291814-1

[12] J. Krawczyk, A. Sobczyk, J. Stryczek, P. Walczak, Tests of new methods of manufacturing elements for water hydraulics. Materials Research Proceedings 5 (2018) 200-205.

[13] M. Hebda, S. Gadek, J. Kazior, Influence of the mechanical alloying process on the sintering behaviour of Astaloy CrM powder mixture with silicon carbide addition. Arch. Metall. Mater. 57 (2012) 733-743. https://doi.org/10.2478/v10172-012-0080-x

[14] A. Szczotok, K. Rodak, Microstructural studies of carbides in MAR-M247 nickel-based superalloy. IOP Conference Series: Materials Science and Engineering 35 (2012) art. 012006. https://doi.org/10.1088/1757-899X/35/1/012006

[15] M. Mazur, K. Mikova, Impact resistance of high strength steels. Materials Today-Proceedings 3 (2016) 1060-1063. https://doi.org/10.1016/j.matpr.2016.03.048

[16] M.S. Kozien, J. Wiciak, Passive structural acoustic control of the smart plate - FEM simulation. Acta Phys. Pol. A 118 (2010) 1186-1188. https://doi.org/10.12693/APhysPolA.118.1186

[17] I. Dominik, J. Kwasniewski, K. Lalik, R. Dwornicka, Preliminary signal filtering in self-excited acoustical system for stress change measurement. CCC 2013 32nd Chinese Control Conf. (2013) 7505-7509.

[18] A. Pacana, M. Pasternak-Malicka, M., Zawada. A. Radon-Cholewa, Decision support in the production of packaging films by cost-quality analysis. Przem. Chem. 95 (2016) 1042-1044.

[19] A. Pacana, K. Czerwinska, R. Dwornicka, Analysis of non-compliance for the cast of the industrial robot basis, METAL 2019 28th Int. Conf. on Metallurgy and Materials (2019), Ostrava, Tanger 644-650. https://doi.org/10.37904/metal.2019.869

[20] T. Lipinski, D. Karpisz, Corrosion rate of 1.4152 stainless steel in a hot nitrate acid. METAL 2019: 28th Int. Conf. on Metallurgy and Materials, Ostrava, TANGER, 2019, 1086-1091. https://doi.org/10.37904/metal.2019.911

[21] A. Gadek-Moszczak, History of stereology. Image Anal. Stereol. 36 (2017) 151-152. https://doi.org/10.5566/ias.1867

[22] A. Gadek-Moszczak, P. Matusiewicz, Polish stereology – a historical review. Image Anal. Stereol. 36 (2017) 207-221. https://doi.org/10.5566/ias.1808

[23] Radek, N., Kurp, P., Pietraszek, J., Laser forming of steel tubes. Technical Transactions 116 (2019) 223-229. https://doi.org/10.4467/2353737XCT.19.015.10055

[24] S. Adamczak, W. Makieła, Analyzing variations in roundness profile parameters during the wavelet decomposition process using the Matlab environment, Metrology and Measurement Systems 1 (2011) 25-34. https://doi.org/10.2478/v10178-011-0003-6